Ultrasensitive Detection of COVID-19 Virus N Protein Based on p-Toluenesulfonyl Modified Fluorescent Microspheres Immunoassay

Mao Mao
Tsinghua University
Feng Wu
Tsinghua University
XueYing Shi
Institute of Biopharmaceutical and Health Engineering, Tsinghua Shenzhen International Graduate School
YuLan Huang
Institute of Biopharmaceutical and Health Engineering, Tsinghua Shenzhen International Graduate School
Lan Ma (malan@sz.tsinghua.edu.cn)
Institute of Biopharmaceutical and Health Engineering, Tsinghua Shenzhen International Graduate School

Research Article

Keywords: COVID-19 N protein, p-toluenesulfonyl, fluorescent microspheres, Lateral flow immunochromatographic assay

Posted Date: January 21st, 2022

DOI: https://doi.org/10.21203/rs.3.rs-1271944/v1

Abstract

The pandemic of new coronary pneumonia caused by the COVID-19 virus continues to ravage the world. Large-scale population testing is the key to controlling infection and related mortality worldwide. Lateral flow immunochromatographic assay (LFIA) is fast, inexpensive, simple to operate, and easy to carry, very suitable for detection sites. This study developed a COVID-19 N protein detect strip based on p-toluenesulfonyl modified rare earth fluorescent microspheres. The p-toluenesulfonyl-activated nanomaterials provide reactive sulfonyl esters to covalently attach antibodies or other ligands containing primary amino or sulfhydryl groups to the nanomaterial surface. Antibodies are immobilized on these nanomaterials through the Fc region, which ensures optimal orientation of the antibody, thereby increasing the capture rate of the target analyte. The use of buffers with high ionic strength can promote hydrophobic binding, in addition, higher pH could promote the reactivity of the tosyl group. The detection limit of the prepared COVID-19 N protein strips can reach 0.01ng/mL so it has great application potential in large-scale population screening.

Introduction

According to WHO data, the cumulative number of confirmed COVID-19 cases reported globally was over 231 million and the cumulative number of deaths was more than 4.7 million until September 28, 2021[1]. Although governments have designated a variety of measures to curb the spread of COVID-19, many countries have encountered severe challenges as the epidemic spreads. More and more countries are experiencing an uncontrollable COVID-19 epidemic, and they desperately need more medical equipment and more extensive testing capabilities. The main symptoms of COVID-19 are respiratory infection-like syndromes: fatigue, dry cough, upper respiratory tract congestion, runny nose, sore throat, myalgia, headache and fever, and diarrhea may occur in a small number of patients. In addition, some patients may have difficulty breathing, while severe COVID-19 patients may rapidly develop acute respiratory distress syndrome, coagulation dysfunction, and septic shock [2].

The pandemic of new coronary pneumonia caused by the SARS-CoV-2 virus continues to ravage the world. Large-scale population testing is needed around the world to successfully control infection and related mortality, which is key to the resumption of all types of products and activities. In this unprecedented medical crisis, to prevent the further expansion of the disease, large-scale and effective detection is particularly important. As a result, the detection technology of COVID-19 has proliferate, researchers around the world have provided more than 200 diagnostic testing methods by 2020 [3]. These innovations have promoted breakthroughs in COVID-19 detection in terms of sensitivity, throughput, and detection time. The current diagnostic tests for COVID-19 are mainly divided into two categories [4]: the detection of viral genetic material (RNA) and the antibodies produced by the human body against viral infections.

Most diagnostic tests for viral RNA are based on reverse transcription-polymerase chain reaction (RT-PCR), a technique considered the gold standard for viral RNA detection [5-7]. RT-PCR technology is highly

sensitive and can amplify minimal amounts of viral RNA, but it also has some disadvantages, such as multiple temperature changes and long detection time. Researchers are seeking answers in other accounting amplification methods to address these issues. For example, the transcription-mediated amplification (TMA), which allows the entire amplification reaction to be carried out in a single reaction tube at constant temperature [8]. In addition, CRISPR technology has also been used to detect the SARS-CoV-2 RNA. This method also uses isothermal amplification and may be used for rapid screening at detection sites [9-11].

Antibody testing uses blood or plasma as a sample to determine the presence of anti-coronavirus antibodies [12,13]. These antibodies are usually immunoglobulin M (IgM) or/and immunoglobulin G (IgG). Specific antibody detection includes enzyme-linked immunosorbent assay (ELISA), lateral flow immunochromatographic assay (LFIA), neutralization test and specific chemical sensors. ELISA is highly efficient and can test multiple samples with high throughput, but its sensitivity varies and it is not suitable for detection sites. By contrast, LFIA detection is fast, cheap, simple to operate, easy to carry, and very suitable for detection sites.

In LFIA technology, it is necessary to couple color probes (nanomaterials) with biomolecules, and the chemical coupling technology is quite classic and perfect [14,15]. For example, the most classic and widely used amide reaction, the amino group on the surface of the antibody and the carboxyl group on the surface of the probe material are biologically coupled under the action of activators and protectors. When nanomaterials and biomolecules are coupled, the distribution and direction of biomolecules on nanomaterials are random, which reduces the coupling efficiency between nanomaterials and biomolecules, and the activity of biomolecules. In organic chemistry, tosyl is a good leaving groups in the nucleophilic substitution (SN2) reaction, and tosylate can also react with other nucleophiles [16]. Tosyl-activated nanomaterials provide reactive sulfonyl esters, and antibodies or other ligands containing primary amino groups or sulfhydryl groups are covalently attached to the surface of the nanomaterials [17]. The antibodies are immobilized on these nanomaterials through the Fc region to ensure the best orientation of the antibodies while increasing the capture rate of target analytes.

In this article, we prepared p-toluenesulfonyl modified fluorescent poly-styrene (PS) microspheres with rare earth fluorescent complexes and used them for the detection of antibodies to the N protein of COVID-19. The COVID-19 fluorescent immunoassay test strips we prepared have high sensitivity and specificity, and can be quickly screened for COVID-19, making them ideal for on-site use.

Materials And Methods

Materials

Europium(III) chloride hexahydrate ($EuCl_3 \cdot 6H_2O$), 2-thenoyltrifluoroacetone (TTA), 1,10-phenanthroline (Phen), N,N-dimethylformamide (DMF), succinic anhydride, styrene (St), methyl methacrylate (MMA), potassium persulfate (KPS), P-toluene sulfonyl chloride (99%),Polyvinylpyrrolidone (K30, Wt. 40000),

Sodium bicarbonate (98%), Sodium dodecyl sulfate (99%), Dichloromethane, Terahydrofuran, N-bromosuccinimide (NBS) and D-(+)-glucose were purchased from Sigma-Aldrich (Shanghai, China). Sodium phosphate dibasic, sodium phosphate monobasic monohydrate, bovine serum albumin (BSA), dimethyl sulphoxide (DMSO) and Tween20 were purchased from Shanghai Sangon Ltd. (Shanghai, China). Gibco® newborn bovine serum were purchased from Thermo Fisher Scientiflc, Inc. (Waltham, MA. U.S.A.). Goat anti-mouse IgG antibody was purchased from Arista Biologicals, Inc. (Allentown, PA. U.S.A.). Styrene and methyl methacrylate were washed using 10% sodium hydroxide solution and deionized water three times before use to remove the inhibitor.

Synthesis of $Eu(TTA)_3Phen$

$Eu(TTA)_3Phen$ was synthesized based on previous studies [18]. Typically, 0.73 g of $EuCl_3·6H_2O$ salt (2 mmol) was dissolved in 20 mL of ethanol in a flask. TTA (6 mmol) and Phen (2 mmol) were dissolved in 20 mL of ethanol in another flask. The $EuCl_3·6H_2O$ salt solution was slowly dropped into the TTA and Phen solution with continuous stirring. The pH value of the solution was adjusted to 7. Then the solution reacted at room temperature for 2 hours. The precipitate produced was washed by ethanol and centrifuged three times at 10000g. The product formed is dried for 12 hours at 60 ℃ in the oven.

Synthesis of p-toluenesulfonyl modified PS microspheres

Briefly, 2 mL styrene and 1 mL MMA were mixed uniformly. Dispersed 0.1 g of p-toluenesulfonyl chloride in 0.5 mL of n-hexane and added to the above mixed solution. After mixing evenly, transferred to a 100 mL three-neck flask and added 50 mL of water. The reaction solution was heated to 80 ℃ after forming a stable microemulsion by ultrasonic treatment, then, 2.5 mL of water containing 0.05 g of potassium persulfate were added. After 10 hours of reaction, the reaction was finished, and the obtained product was centrifuged to remove impurities, and dispersed in water for later use.

Synthesis of fluorescent PS microspheres

We used the swelling method to prepare fluorescent PS microspheres. Generally, 2 mL of the p-toluenesulfonyl modified PS microspheres obtained earlier, added 8 mL of water, 0.1 g PVP, 0.1 g SDS and 0.01 g $NaHCO_3$ to dissolve the solids for use. 0.04 g $Eu(TTA)_3Phen$ dispersed in 1.67 mL dichloromethane, then added 0.083 mL tetahydrofuran and mix well. Added the mixture to the aqueous solution and stirred under airtight conditions for two hours, then opened the lid and continued stirring for 22 hours. The obtained product was centrifuged to remove impurities, and dispersed in water for later use.

Preparation of COVID-19 N protein monoclonal antibody

Prepared COVID-19 N protein monoclonal antibody based on previous research [19].

Preparation of p-toluenesulfonyl modified fluorescent PS microspheres antibodies conjugates

After washing with 0.1M borate buffer (pH=9.5), an appropriate amount of p-toluenesulfonyl fluorescent microspheres were dispersed into 66.6 μL borate buffer (pH = 8.5) to obtain reaction solution 1. Mixed 0.1 M borate buffer (pH = 8.5) and 0.3 M $(NH_4)_2SO_4$ solution uniformly, and then added the labeled antibody to obtain reaction solution 2. 33.3 μL reaction solution 2 was added to reaction solution 1 and incubated at 37 ℃ for 4 hours. It was then washed twice in PBS (phosphate buffered saline) containing 0.5% BSA and incubated in PBS containing 0.5% BSA in 1mL for 1 hour at 37 °C. The fluorescent microspheres were then washed twice in PBS containing 0.1% BSA and reconstituted in 1 mL PBS containing 0.1% BSA for storage.

Preparation of p-toluenesulfonyl fluorescent microspheres immunochromatographic assay test strips

The anti-COVID-19 N protein antibody was diluted with 20 mM PBS buffer (pH = 7.4), the detection line was drawn on the nitrocellulose membrane at a concentration of 1.5 mg/mL using the XYZ distribution system (BioDot Inc, Irvine, CA). Then the goat anti-mouse IgG antibody was delimited on the nitrocellulose membrane at 1 mg/mL concentration as the quality control line. The nitrocellulose membrane was dried at 37°C for 4 hours. The sample pad was saturated with PBS buffer containing BSA (1%, w/v) and Tween-20 (0.1%, w/v), and dried at 37°C for 3 hours after treatment. After the nitrocellulose membrane was dried, the antibody-labeled fluorescent microspheres were sprayed onto the sample pad, and finally the fluorescent microsphere-LFIA test strips were assembled according to the standard, and cut into individual 3.5 mm wide test strips using CM4000 Guillotine Cutter (BioDot Inc., Irvine, CA).

Analytical procedure

60 μL COVID-19 standard samples with different concentrations were added to the sample pads on the fluorescent microsphere-LFIA test strips for 15 minutes. Then scanned with the fluorescence test strip scanner to get the fluorescence signal intensity on the strip. Precisely, when the COVID-19 N protein was present in the sample, it could specifically bind to the antibody-labeled fluorescent microspheres prepared before, and then be captured by the coated antibody at the detection line to form a sandwich structure to generate a fluorescent signal. Conversely, if there was no COVID-19 heavy N protein in the test sample, the antibody-labeled fluorescent microspheres would be captured by the goat anti-mouse antibody at the quality control line, and there would be no fluorescent signal at the test line. When the fluorescent microspheres were captured, a bright fluorescent band appeared under the ultraviolet (UV) lamp of 365 nm, and its fluorescence intensity was proportional to the number of antigens captured.

Results And Discussion

Properties of p-toluenesulfonyl modified PS microspheres

The microemulsion polymerization method is used to prepare polystyrene microspheres. During the growth of polystyrene microspheres, due to the presence of p-toluene sulfonyl chloride in the oil droplets, it will react with the hydroxyl groups on the surface of the polystyrene microspheres to finally obtain p-

toluenesulfonyl modified PS microspheres, and the pH of the solution will become acidic. The reaction process is shown in Figure 1A.

In figure 2, FT-IR spectroscopy shows the characteristic frequency of the copolymerization of styrene, methyl methacrylate and the p-toluenesulfonyl group. The peak position at 1727cm^{-1} is the C=O stretching vibration of carboxylic acid carbonyl; the peak position at 1180cm^{-1} is the symmetrical stretching vibration of sulfonyl chloride O=S=O and the peak at 1380cm^{-1} is sulfonyl chloride O=S=O antisymmetric stretching vibration.

Properties of fluorescent PS microspheres

Fluorescent PS microspheres with a similar core-shell structure are prepared by a swelling method, and their TEM (Transmission electron microscope) images are shown in figure 3A. Figure 3B shows the appearance of the fluorescent PS microspheres under natural light and 360nm ultraviolet irradiation. Under 365nm ultraviolet light irradiation, the fluorescent PS microspheres emit bright red light. It is worth noting that the shell thickness of fluorescent PS microspheres increases gradually with increasing the amount of p-Toluenesulfonyl chloride. The amount of p-toluenesulfonyl chloride added in Fig. 3C are 5 times that in Fig. 3A, and it is obvious that the thickness of the shell layer has increased a lot.

As can be seen from Figure 4 that when $Eu(TTA)_3Phen$ is swelled into the p-toluenesulfonyl modified PS microspheres, there is almost no difference in optical properties between fluorescent microspheres and Eu $(TTA)_3Phen$, which shows that this method can ensure the optical properties of the fluorescent material as much as possible.

Properties of p-toluenesulfonyl fluorescent microspheres immunochromatographic assay test strips

The standard sample of COVID-19 N protein was used for the analysis of the performance of the LFIA strips. To verify the availability of the strips, the strip was scanned by fluorescence test strip scanner after 15 min of adding the samples. We detected a series of different concentrations of COVID-19 N protein standards. The COVID-19 N protein standards were diluted in NBS to obtained 0, 0.001, 0.01, 0.1, 1, 10, 100, 1000 ng/mL samples respectively. The samples of each concentration were tested three times, and the average values were calculated. The results obtained are given in figure 5. With the concentration increasing, the fluorescence signals on the test line of LFIA strips were still visible at 0.01 ng/mL. After testing, the limit of detection (LOD) of COVID-19 N protein LFIA strips is 0.01 ng/mL, and the linearity range is 0.01~10 ng/mL. Particularly, if the concentration of standards was over a critical concentration (10 ng/mL), the hook effect would lead to an obvious fluorescence signal interference.

Specificity of COVID-19 N protein LFIA strips

HCoV-229E, HCoV-OC43, HCoV-NL63, HCoV-HKU1, influenza A H1N1, influenza A H3N2, influenza A H5N1, influenza A H7N9, influenza A H9N2, influenza B Victoria strain, influenza B Yamagata strain, Measles virus, Mumps virus, Rubella virus, Varicella zoster virus, Staphylococcus aureus, Pseudomonas

aeruginosa, SARS-CoV N protein and MERS-CoV N protein were used to evaluate the specificity of COVID-19 N protein LFIA strips respectively. After testing, the COVID-19 N protein LFIA strips do not cross-react with other myocardial infarction markers (Fig. 6).

At present, there are many methods for coupling nanomaterials to biomolecules, of which chemical-based labeling techniques are quite classic and perfect. These chemical-based labeling techniques cover a wide range and are applicable to native proteins. Chemical reactive functional groups are exposed on the surface of all natural proteins, such as thiol (Cys), amine (Lys), carboxyl (Asp, Glu), hydroxyl (Ser, Thr, Tyr), guanidine (Arg), imidazole (His), and indole (Trp), which can be modified by traditional chemical reactions. For example, thiol coupling reactions such as Cys-maleimide and amine (Lys) coupling reactions with active esters or isocyanates are widely used. One of the fatal drawbacks of these chemical-bioconjugation methods [14,15] is their low selectivity in targeting many other proteins and/or modifying specific sites in the target protein. Traditional chemical labeling methods, such as the amide reaction between amino and carboxyl groups, require the addition of N-Hydroxy succinimide (NHS) and 1-(3-Dimethylaminopropyl)-3-ethylcarbodiimide hydro (EDC) as activators and protectors, and when nanomaterials are coupled with biomolecules, the distribution and orientation of biomolecules on nanomaterials are random. More importantly, these problems reduce the coupling efficiency between materials and biomolecules, as well as the activity of biomolecules.

Protein affinity labeling based on ligand-directed chemistry has been widely used to specifically label native proteins. In this approach, an optical or chemical reaction handle is attached to a ligand, such as a drug or natural product that can specifically bind to the target protein. The ligand-protein interaction then promotes protein labeling in the environment with greater specificity. Although this technique can be used to identify and characterize ligand-specific target proteins, it often suffers from low yields of cross-linked products. Recent advances in affinity labeling using proximity-driven nucleophilic reactions with moderate reactivity have provided reasonably high yields [20].

In organic chemistry, the tosyl group is one of the good leaving groups for nucleophilic substitution (SN2) reactions. Tosylates can also react with other nucleophiles, such as hydroxyl groups (such as alkoxides, RO-) to form ether bonds under higher pH conditions, thiols (such as thiolate anions RS-) to form thioether bonds, and OH- in alkaline conditions, which would result in the hydrolysis of OH- back to the hydroxyl group. Reaction with these groups under non-aqueous conditions requires organic bases as proton acceptors to catalyze the coupling [16]. Tosyl-activated nanomaterials provide reactive sulfonyl esters to covalently attach antibodies or other ligands containing primary amino or sulfhydryl groups to the nanomaterial surface (Fig. 1 (B)). Antibodies are immobilized on these nanomaterials via the Fc region, which ensures optimal orientation of the antibody, thereby increasing the capture rate of the target analyte [17]. The physical adsorption of antibodies to nanomaterials is rapid, however, the formation of covalent bonds therein takes a relatively long time. To improve coupling efficiency, buffers with high ionic strength should be used because they promote hydrophobic binding. Also, the tosyl group is more reactive at higher pH, so sodium borate buffer (pH 9.5) should be used.

By comparison, our work proved that the nucleocapsid antigen-monoclonal antibody (mAbs) system was more suitable for the immunodetection of the COVID-19. On this basis, a rapid test strip was developed for mass screening of COVID-19 population. This kind of test strip uses colloidal gold as a probe, and its detection limit is 0.1ng/mL [19]. In this article, we used p-toluenesulfonyl modified fluorescent microspheres as fluorescent probes. The p-toluenesulfonyl group improves the coupling efficiency of fluorescent probes and antibodies, eliminating the need for NHS and EDCs as activators and protectors, thus simplifying the reaction steps. Table 1 shows the fluorescence signal intensities of the detection lines on the COVID-19 N protein LFIA strips using the fluorescence test strip scanner to detect different concentrations of COVID-19 N protein standard samples. Obviously, a fluorescence signal that is significantly different from the background noise can be observed on the strip with the standard concentration of 0.01ng/mL. This proves that the detection limit of the prepared test strip is 0.01 ng/mL, which is 10 times higher than the previous work. In order to further study of quantitative measurement of N proteins, the concentration of N proteins and the corresponding fluorescence intensity were well fitted by the nonlinear equation. The variables satisfy the Logistic function model, the confident function expression is as follow: , the associated parameters were shown in Fig. 7. At the same time, the test strip has good specificity, and these advantages make the test strip have great potential in the application of large-scale population screening for COVID-19.

Table 1. The fluorescence signal intensities of the detection lines on the COVID-19 N protein LFIA strips with different concentrations of COVID-19 N protein standard samples.

Concentration (ng/mL)	TEST1	TEST2	TEST3	Average	STDEV
1000	19252	20629	20582	20154.33	781.7969
100	20498	20678	20526	20567.33	96.85728
10	20910	21133	21172	21071.67	141.3589
1	6102	6493	6490	6361.667	224.8829
0.1	1294	1362	1285	1313.667	42.09909
0.01	872	896	804	857.3333	47.72141
0.001	368	400	365	377.6667	19.39931
0	265	254	344	287.6667	49.09515

Conclusion

In this study, p-Toluenesulfonyl modified rare earth fluorescent microspheres were prepared by a swelling method. After p-toluenesulfonyl activates the fluorescent probe, the Fc region of the antibody will be coupled to the surface of the fluorescent probe, thereby ensuring the orientation of the antibody biomolecules on the surface of the nanomaterial, which can effectively improve the coupling efficiency. When the pH value is higher, the coupling efficiency will be higher. After that, a COVID-19 N protein detect

strip was prepared, which has the advantages of fast detection speed, good specificity and high sensitivity, and has great potential in the application of large-scale screening of COVID-19 population.

Abbreviations

LFIA: lateral flow immunochromatographic assay

RT-PCR: reverse transcription-polymerase chain reaction

TMA: transcription-mediated amplification

IgM: immunoglobulin M

IgG: immunoglobulin G

ELISA: enzyme-linked immunosorbent assay

$EuCl_3 \cdot 6H_2O$: Europium (III) chloride hexahydrate

TTA: 2-thenoyltrifluoroacetone

Phen: 1,10-phenanthroline

DMF: N,N-dimethylformamide

St: styrene

PS: poly-styrene

MMA: methyl methacrylate

KPS: potassium persulfate

PVP: Polyvinylpyrrolidone

SDS: Sodium dodecyl sulfate

BSA: bovine serum albumin

DMSO: dimethyl sulphoxide

PBS: phosphate buffered saline

UV: ultraviolet

FT-IR: fourier transform infrared spectroscopy

TEM: transmission electron microscope

NBS: n-bromosuccinimide

LOD: limit of detection

NHS: N-Hydroxy succinimide

EDC: 1-(3-Dimethylaminopropyl)-3-ethylcarbodiimide hydro

mAbs: antigen-monoclonal antibody

Declarations

Ethics declarations

Balb/C mice were kept in a pathogen-free environment and ad-lib fed. The procedures for care and use of animals were approved by the Ethics Committee of the International Graduate School at Shenzhen, Tsinghua University and all applicable institutional and governmental regulations concerning the ethical use of animals were followed.

Author Contributions

Conceptualization, LM; methodology, MM; investigation, MM; data curation, MM and FW; writing—original draft preparation, XYS and YLH helped in performing experiments and preparing monoclonal antibodies, MM and LM; supervision, LM; funding acquisition, LM. All authors have read and agreed to the published version of the manuscript.

Funding

This work was supported by the National Key R & D Plan in China (2020YFA0908900). Shen zhen Science and Technology research and development funds (JCYJ20200109143018683). State Key Laboratory of Chemical Oncogenomics, Institute of Biomedical Health Technology and Engineering, Shenzhen Bay Laboratory.

Competing interests

The authors declare that they have no competing interests.

Acknowledgements

We thank the reviewers for their valuable comments.

Availability of data and materials

All data generated or analyzed during this study are included within the article.

References

1. https://www.who.int/publications/m/item/weekly-epidemiological-update-on-covid-19---28-september-2021.
2. Chang D, Lin M, Wei L, Xie L, Zhu G, Dela Cruz, C S, Sharma L (2020) Epidemiologic and clinical characteristics of novel coronavirus infections involving 13 patients outside Wuhan. China. JAMA. 323, 1092–1093. https://doi.org/10.1001/jama.2020.1623.
3. Linda J. Carter, Linda V. Garner, Jeffrey W. Smoot, Yingzhu Li, Qiongqiong Zhou, Catherine J. Saveson, Janet M. Sasso, Anne C. Gregg, Divya J. Soares, Tiffany R. Beskid, Susan R. Jervey and Cynthia Liu (2020) Assay Techniques and Test Development for COVID-19 Diagnosis. ACS Cent. Sci. 6, 591–605. https://pubs.acs.org/doi/10.1021/acscentsci.0c00501
4. Jones H (2020) The Importance of diagnostic testing for COVID-19. Infectious Diseases Hub; April 2. https://www.id-hub.com/2020/04/02/the-importance-of-diagnostic-testing-for-covid-19/
5. Xia J, Tong J, Liu M, Shen Y, Guo D (2020) Evaluation of coronavirus in tears and conjunctival secretions of patients with SARS-CoV-2 infection. J. Med. Virol. 92, 589–594. https://www.ncbi.nlm.nih.gov/pmc/articles/PMC7228294/
6. American College of Physicians (2020) COVID-19 found in sputum and feces samples after pharyngeal specimens no longer positive. Science Daily; March 30. https://www.sciencedaily.com/releases/2020/03/200330110348.htm
7. Kujawski SA, Wong KK, Collins JP (2020) Clinical and virologic characteristics of the first 12 patients with coronavirus disease 2019 (COVID-19) in the United States. Nat. Med. 26, 861–868. https://www.nature.com/articles/s41591-020-0877-5.
8. Kacian DL, Fultz TJ (1999) Kits for nucleic acid sequence amplification methods. U.S. Patent 4888779.
9. What is CRISPR? Ask the Brain, (January 1, 2019) The McGovern Institute for Brain Research, Massachusetts Institute of Technology. https://mcgovern.mit.edu/ask-the-brain/
10. Zhang F, Abudayyeh OO, Gootenberg JS. A protocol for detection of COVID-19 using CRISPR diagnostics (v.20200321). Broad Institute of MIT and Harvard. www.broadinstitute.org/files/publications/special/COVID19%20detection%20(updated).pdf.
11. James P. Broughton, Xianding Deng, Guixia Yu, Clare L. Fasching, Venice Servellita, Jasmeet Singh, Xin Miao, Jessica A. Streithorst, Andrea Granados, Alicia Sotomayor-Gonzalez, Kelsey Zorn, Allan Gopez, Elaine Hsu, Wei Gu, Steve Miller, Chao-Yang Pan, Hugo Guevara, Debra A. Wadford, Janice S. Chen & Charles Y. Chiu (2020) CRISPR–Cas12-based detection of SARS-CoV-2. Nat. Biotechnol, 38, 870–874. DOI: 10.1038/s41587-020-0513-4.
12. Saahir Khan, Rie Nakajima, Aarti Jain, Rafael Ramiro de Assis, Al Jasinskas, Joshua M Obiero, Oluwasanmi Adenaiye, Sheldon Tai, Filbert Hong, Donald K Milton, Huw Davies, Philip L Felgner,

Prometheus Study Group (2020) Analysis of serologic cross-reactivity between common human coronaviruses and SARS-CoV-2 using coronavirus antigen microarray. bioRxiv, 2020.03.24.006544. DOI: 10.1101/2020.03.24.006544.

13. Bo Diao, Kun Wen, Jian Chen, Yueping Liu, Zilin Yuan, Chao Han, Jiahui Chen, Yuxian Pan, Li Chen, Yunjie Dan, Jing Wang, Yongwen Chen, Guohong Deng, Hongwei Zhou, Yuzhang Wu (2020) Diagnosis of acute respiratory syndrome coronavirus 2 infection by detection of nucleocapsid protein. medRxiv, 2020.03.07.20032524. DOI: 10.1101/2020.03.07.20032524.
14. Sletten, E.M. and Bertozzi, C.R. (2009) Bioorthogonal chemistry: fishing for selectivity in a sea of functionality. Angewandte Chemie International Edition, 48 (38), 6974–6998. https://doi.org/10.1002/anie.200900942.
15. Takaoka Y, Ojida A, and Hamachi I. (2013) Protein organic chemistry and application for labeling and engineering in live-cell systems. Angewandte Chemie International Edition, 52 (15), 4088–4106. https://onlinelibrary.wiley.com/doi/10.1002/anie.201207089
16. Carey FA, Sundberg RJ, (2007) Conversion of alcohols to alkylating agents; sulfonate esters Advanced Organic Chemistry, Part B: Reactions and Synthesis, Fifth ed., Springer Science + Business Media, New York, NY. p. 216.
17. BA Otieno, CE Krause, JF Rusling (2016) Bioconjugation of Antibodies and Enzyme Labels onto Magnetic Beads. Methods in Enzymology, 571:135-50. Doi: 10.1016/bs.mie.2015.10.005.
18. Feng Wu, Mao Mao, Yu Cen, Hongtian Yang, Zhifeng Qin and Lan Ma (2017) Copolymerization of $Eu(TTA)_3Phen$ doped styrene and methyl methacrylate nanoparticles and use in quantitative detection of pepsinogen. RSC Adv. 7, 12217. https://doi.org/10.1039/C6RA27071A
19. Dan Liu, Feng Wu, Yu Cen, Lei Ye, Xueyin Shi, Yulan Huang, Shisong Fang, Lan Ma (2021) Comparative research on nucleocapsid and spike glycoprotein as the rapid immunodetection targets of COVID-19 and establishment of immunoassay strips. Molecular Immunology, 131, 6–12. DOI: 10.1016/j.molimm.2021.01.005
20. Chen, G., Heim, A., Riether, D., Yee, D., Milgrom, Y., Gawinowicz, M.A., and Sames, D. (2003) Reactivity of functional groups on the protein surface: development of epoxide probes for protein labeling. Journal of the American Chemical Society, 125 (27), 8130–8133. DOI: 10.1021/ja034287m.

Figures

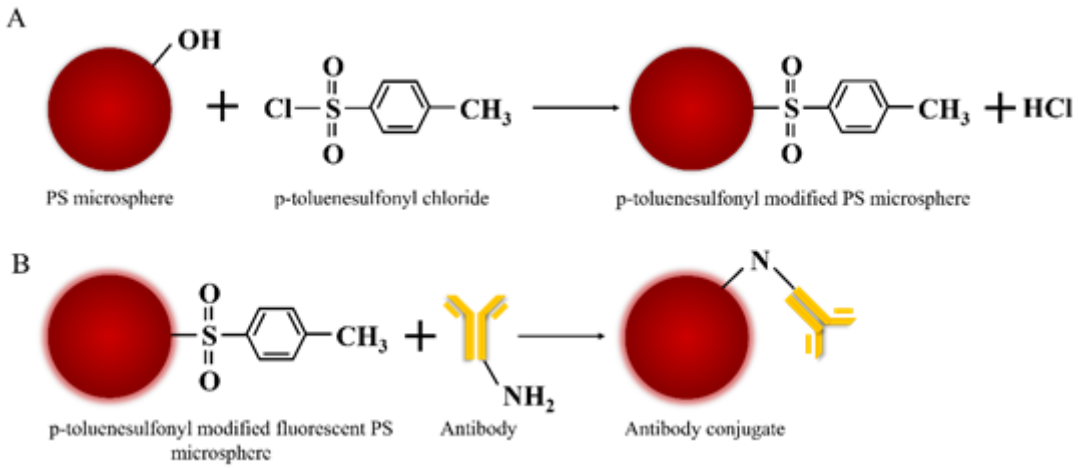

Figure 1

(A) Schematic diagram of p-toluenesulfonyl modified PS microspheres. (B) Conjugation of antibodies to p-toluenesulfonyl modified fluorescent PS microspheres.

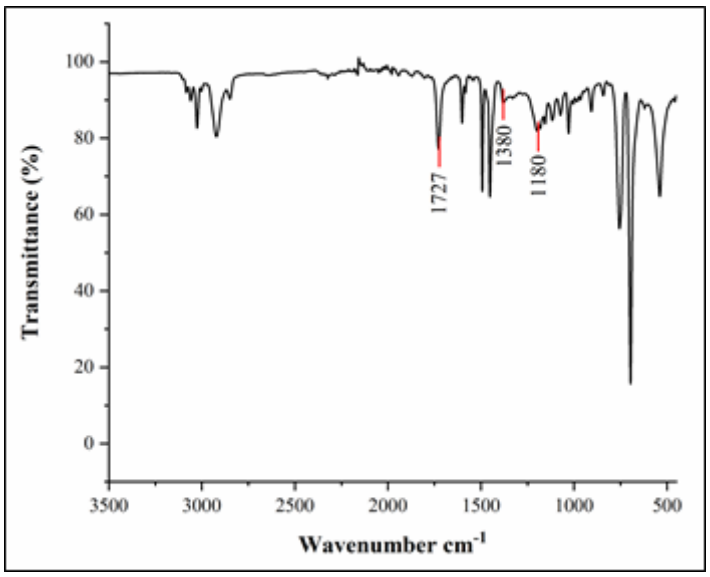

Figure 2

FT-IR spectroscopy of p-toluenesulfonyl modified PS microspheres

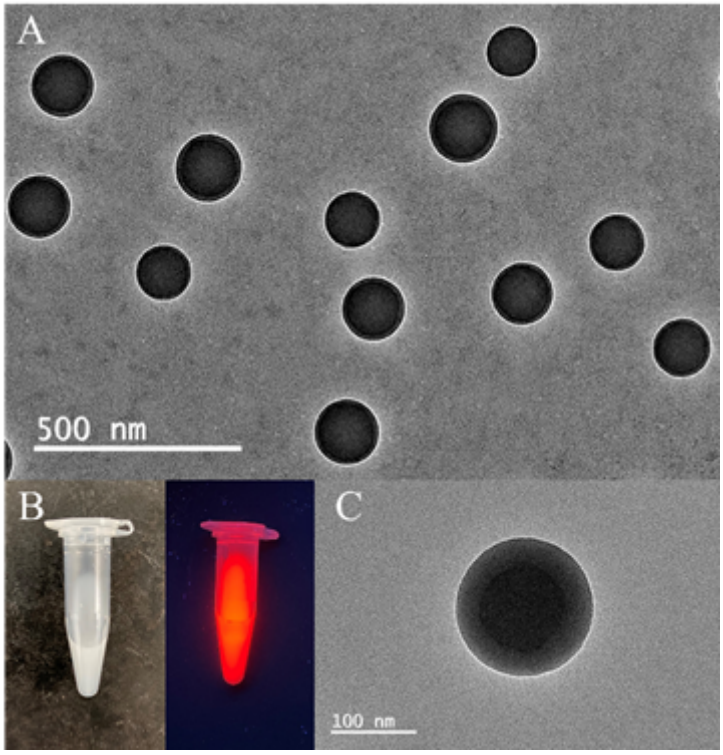

Figure 3

(A) TEM image of fluorescent PS microspheres. (B) Photograph of fluorescent PS microspheres under natural light and 365 nm ultraviolet light. (C) TEM image of fluorescent PS microspheres with 5 times the amount of p-toluenesulfonyl chloride

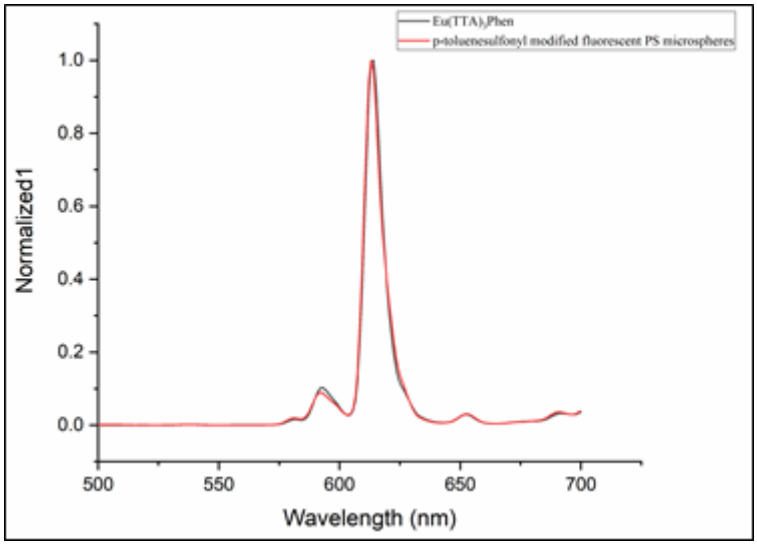

Figure 4

Fluorescence spectra of $Eu(TTA)_3Phen$ and fluorescent PS microspheres.

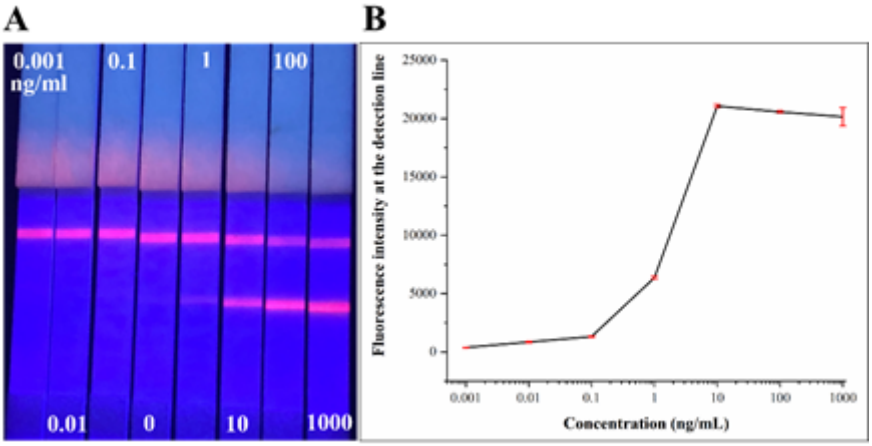

Figure 5

The test results of COVID-19 N protein standards using LFIA strips. (A) Images of corresponding concentrations tested COVID-19 N protein LFIA strips under 365 nm ultraviolet light. (B) Different concentrations of COVID-19 N protein standards measured by the fluorescence strip scanning device.

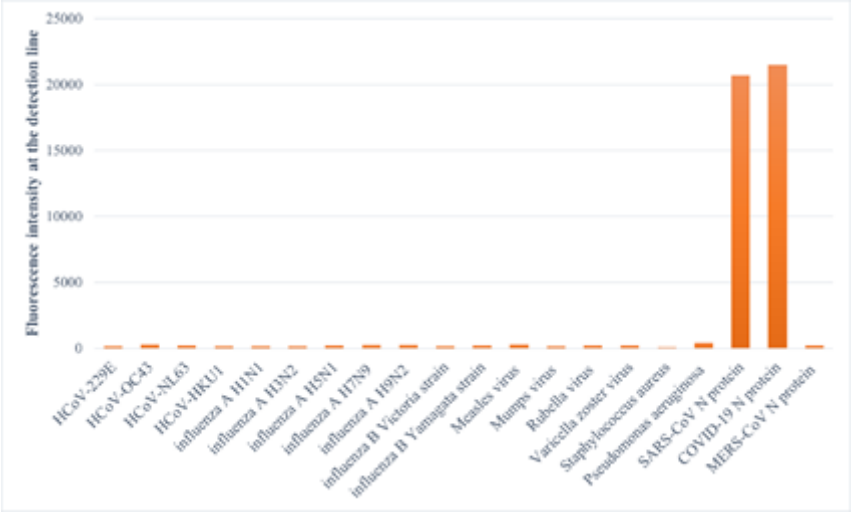

Figure 6

Specificity test results of COVID-19 N protein LFIA strips

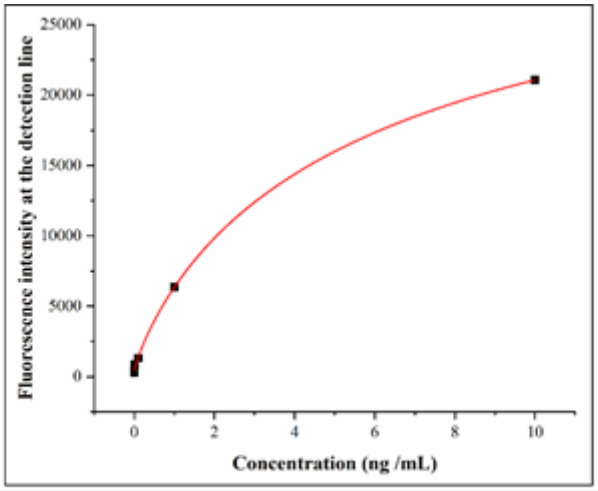

	A1	A2	x0	p	Function	R^2
N protein	429.09	35051.21	6.34	0.85	y = A2 + (A1-A2)/(1 + (x/x0)^p)	0.99965

Figure 7

The COVID-19 N protein LFIA strips parameters and function of fitting nonlinear equation between concentration and fluorescence intensity of N proteins.